Title

Controlling the Release of Small, Bioactive Proteins via Dual Mechanisms with Therapeutic Potential

Journal

Advanced Healthcare Materials, 6(24)

ISSN

2192-2640

Authors

Kharkar, Prathamesh M

Scott, Rebecca A

Olney, Laura P

et al.

Publication Date

2017-12-01

DOI

10.1002/adhm.201700713

Peer reviewed

HHS Public Access

Author manuscript

Adv Healthc Mater. Author manuscript; available in PMC 2018 December 01.

Published in final edited form as:

Adv Healthc Mater. 2017 December ; 6(24): . doi:10.1002/adhm.201700713.

Controlling the release of small, bioactive proteins via dual mechanisms with therapeutic potential

Prathamesh M. Kharkar[‡], **Rebecca A. Scott**[‡,§,**], **Laura P. Olney**[#,**], **Paige J. LeValley**[†,**], **Emanual Maverakis**[#], **Kristi L. Kiick**[⊥,*], and **April M. Kloxin**[‡,†,*]

[‡]Department of Materials Science and Engineering, University of Delaware, 201 DuPont Hall, Newark, Delaware 19716, United States

[§]Nemours - Alfred I. duPont Hospital for Children, 1600 Rockland Road, Wilmington, Delaware 19803

[#]Department of Dermatology, School of Medicine, University of California, Davis, California

[†]Department of Chemical and Biomolecular Engineering, University of Delaware, 150 Academy Street, Newark, Delaware 19716, United States

[⊥]Delaware Biotechnology Institute, University of Delaware, 15 Innovation Way, Newark, DE 19711

Abstract

Injectable drug delivery systems that respond to biologically relevant stimuli present an attractive strategy for tailorable drug delivery. Here, we report the design and synthesis of unique polymers for the creation of hydrogels that are formed *in situ* and degrade in response to clinically relevant endogenous and exogenous stimuli, specifically reducing microenvironments and externally applied light. Hydrogels were formed with polyethylene glycol and heparin-based polymers using a Michael-type addition reaction. The resulting hydrogels were investigated for the local controlled release of low molecular weight proteins (e.g., growth factors and cytokines), which are of interest for regulating various cellular functions and fates *in vivo* yet remain difficult to deliver. Incorporation of reduction-sensitive linkages and light-degradable linkages afforded significant changes in the release profiles of fibroblast growth factor-2 (FGF-2) in the presence of the reducing agent glutathione or light, respectively. The bioactivity of the released FGF-2 was comparable to pristine FGF-2, indicating the ability of these hydrogels to retain the bioactivity of cargo molecules during encapsulation and release. Further, *in vivo* studies demonstrated degradation-mediated release of FGF-2. Overall, our studies demonstrate the potential of these unique stimuli-responsive chemistries for controlling the local release of low molecular weight proteins in response to clinically relevant stimuli.

Keywords

injectable hydrogel; controlled release; biologics delivery; responsive materials

[*] akloxin@udel.edu (AMK), kiick@udel.edu (KLK).

[**] equal contribution

1. Introduction

Injectable hydrogels are of continued and growing interest in a variety of biomedical settings, from delivery of cancer therapeutics to applications in regenerative medicine. Hydrogels with high loading capacity can locally deliver bioactive cargoes (e.g., proteins and cells) with varying degrees of tunable release based on their material design. Physical hydrogels formed by intermolecular interactions (e.g., ionic, hydrophobic, hydrogen bonding) between engineered peptides, proteins, or polymers have been foundational, owing to their ease of injection and potential for relevant biochemical interactions with cargoes (e.g., affinity binding).[1] While effective for injection, these materials often have weak mechanical properties relative to tissues and limited control of hydrogel dissolution and cargo release.[2] Covalent hydrogels utilizing click chemistries also have been deployed in select cases, where choice of functional groups (e.g., thiol-maleimide, aldehyde-hydrazide) and solution conditions allow for *in situ* formation upon mixing and injection.[1, 3] Degradation and release from these mechanically-robust materials have been controlled by the incorporation of cleavable moieties. Additionally, dynamic covalent chemistries have been reported recently, where reversible covalent bonds enable shear-thinning for facile injection as well as responsive dissolution and cargo release.[4] However, challenges remain in achieving controlled *and* tailored release profiles of small bioactive proteins toward regulating complex biological processes (e.g., signaling cascades in wound healing and immune activation).[5]

Several hydrogel-based drug carriers, such as bulk hydrogels, nanogels, liposomes, and nanoparticles, have been employed for the delivery of small bioactive proteins.[6] For example, for intracellular delivery, Zhong and coworkers established hyaluronic acid nanogels that degrade in response to reducing microenvironments through disulfide bonds and subsequently release cytochrome *c* and granzyme B for the treatment of lung carcinoma.[7] For extracellular delivery, Burdick and coworkers demonstrated that injectable polysaccharide-based hydrogels that degrade in response to matrix metalloproteinases (MMPs) could be utilized to release a tissue inhibitor of MMPs to modulate cellular activity during the wound healing cascade following myocardial infarction.[8] Building upon these advances, we hypothesized that noncovalent protein-polysaccharide interactions in conjunction with controlled hydrogel degradation in response to endogenous and exogenous stimuli would afford precise control over the release kinetics of low molecular weight proteins, such as growth factors and cytokines, ranging from a few days to weeks *in vitro* and *in vivo*.

In the work presented herein, we demonstrate the design, synthesis, and application of an injectable hydrogel-based material for the responsive and tailorable release of small bioactive proteins with broad applicability toward the *in situ* modulation of biological processes in regenerative medicine and disease treatment. To enable hydrogel formation as well as degradation in response to endogenous stimuli, we incorporated an aryl-thiol based crosslinker to form succinimide thioether linkages that are susceptible to thiol exchange reactions in glutathione (GSH)-rich reducing microenvironments, such as those found within carcinoma tissue. In addition, to enable degradation that can be tailored with exogenous stimuli, we synthesized a new *o*-nitrobenzyl (*o*-NB) aryl-thiol moiety that is responsive to

externally applied, cytocompatible doses of light. Both macromers were designed free of ester bonds to mitigate material degradation by hydrolysis and allow precise and responsive control of degradation reactions and hydrogel dissolution. For the retention of small bioactive proteins, such as basic fibroblast growth factor (FGF-2), interleukin-2 (IL-2), or vascular endothelial growth factor (VEGF), heparin crosslinks were incorporated to promote electrostatic protein-polysaccharide binding. The rate and extent of hydrogel degradation with different stimuli and degradable content were characterized using oscillatory rheometry. These handles for modulation of hydrogel degradation subsequently were utilized to control the release of a model bioactive protein FGF-2 (~17.2 kDa), which is a potent mitogen that plays an important role in cell proliferation, migration, and wound healing.[9] Stimuli-responsive release of FGF-2 was investigated *in vitro* and *in vivo*, and retention of protein bioactivity was verified. This materials system and approach can easily be applied for local, tailored delivery of other low molecular weight proteins with heparin affinity, such as IL-2 for melanoma treatment or VEGF for regenerative medicine applications.

2. Results and Discussion

2.1 Materials design and synthesis

Hydrogels based on poly(ethylene glycol) (PEG) are well suited for drug delivery applications owing to their excellent biocompatibility, their tunable mechanical properties, and the ease of control over their chemical modification.[5, 10] The release of cargo from PEG-based hydrogels generally is controlled by Fickian diffusion (e.g., encapsulation of protein and release by passive or hindered diffusion), material degradation (e.g., entrapment of protein and release upon crosslink cleavage), or a combination of both. The incorporation of natural polymers (e.g., polysaccharides such as heparin) within hydrogels allows for non-covalent interactions with biological cargo, which both improve the stability of cargo molecules during the encapsulation process and the control of cargo release kinetics.[11] The heterogeneity of the glycosaminoglycan heparin, coupled with its highest negative charge density among naturally occurring polymers, facilitates ionic interactions with a wide variety of proteins, growth factors, and cytokines.[12] Hence, we hypothesized that a hydrogel incorporating different endogenous and exogenous stimuli-responsive moieties and heparin would afford control over the release of low molecular weight protein cargo by a combination of heparin-mediated interactions and degradation-mediated changes in mesh size (Fig. 1).

We aimed to design building blocks for the formation of water-stable hydrogels that are degradable exclusively by responsive mechanisms using amide linkages rather than esters, owing to their long-term stability in aqueous microenvironments. Building upon our prior success with aryl-thiol-based thioether succinimide linkages for GSH-responsive release,[13, 14] we conjugated aryl-thiol groups to amine-end-functionalized PEG (PEG-4-NH_2) using carbodiimide chemistry (Fig. 1B). Direct addition of mercaptophenylacetic acid (MPA) to PEG-4-NH_2 was challenging due to the formation of thioester linkages (i.e., reaction of the sulfhydryl groups with the carboxylic acids), which are unstable under aqueous conditions. Hence, MPA was first oxidized using hydrogen peroxide (H_2O_2) in the presence of sodium iodide (NaI) as a catalyst to form disulfide bonds that prevent the

participation of sulfhydryl groups in subsequent reactions with activated carboxylic acids. The carboxylic acid groups on the oxidized MPA were activated with 1-[bis(dimethylamino)methylene]-1H-1,2,3-triazolo[4,5-b]pyridinium 3-oxid hexafluorophosphate (HATU) in the presence of N,N-diisopropylethylamine (DIPEA) to form an amide linkage with PEG-4-NH_2. Successively, the polymer was reduced in the presence of tris(2-carboxyethyl)phosphine (TCEP) to generate reactive sulfhydryl groups in acidic conditions (pH ~ 4). The reaction yielded aryl-thiol end-functionalized polymers with 88% modification as assessed by the integration of aromatic protons within the ^{1}H NMR spectrum (Figure S1).

To enable exogenously triggered, light-mediated degradation of the hydrogels, an *o*-NB moiety was incorporated within PEG-4-MPA (Fig. 1B). The *o*-NB moiety undergoes irreversible photoisomerization in response to externally applied cytocompatible doses of light.[15] In our previous work, we incorporated an ester-linked maleimide *o*-NB moiety onto a four-arm PEG macromer;[13] however, this formulation presented challenges due to hydrolysis of the maleimide ring during monomer synthesis in addition to the rapid hydrolysis ($k = 6.84 \times 10^{-4}$ min^{-1}) of esters within the resulting hydrogels in aqueous solution. To address these issues, a new amide-linked MPA *o*-NB was synthesized on PEG-4-NH_2 (Scheme S1). Amine end-functionalized PEG (**I**) was reacted with the carboxylic acid of Fmoc-protected *o*-NB groups (**II**) using carbodiimide chemistry. Subsequently, the Fmoc protecting group on the photodegradable PEG (**III**) was cleaved in the presence of piperidine to generate an amine end-functionalized photodegradable PEG intermediate (**IV**). Intermediate IV was reacted with oxidized MPA in a similar manner as described earlier to obtain aryl-thiol end-functionalized photodegradable PEG (PEG-4-PD-MPA) with 78% modification, as indicated by ^{1}H NMR (Figure S3). To the best of our knowledge, this is the first reported synthesis of an aryl-thiol end-functionalized photodegradable PEG macromer for controlling hydrogel degradation.

To enable the retention of small proteins with affinity binding, heparin was functionalized with maleimide groups for incorporation as crosslinks within the responsive hydrogels (Fig. 1C). Heparin- and heparin-sulfate-based polymers have been utilized in a variety of hydrogels for controlling the release of proteins with receptor-ligand interactions.[16] The large electronegative charge of heparin[12] facilitates its role in multivalent binding of many proteins, including FGF-2 (k_d = 0.47 μM),[17] IL-2 (k_d = 0.5 μM),[18] and VEGF (k_d = 0.52 μM).[19] Here, the carboxylic acid groups on uronic acid residues of heparin were functionalized with maleimide groups using a heterofunctional N-(2-aminoethyl) maleimide trifuoroacetate salt (AEM) and carbodiimide coupling chemistry (Scheme S2). Optimization of the reactant stoichiometry for the carbodiimide reaction yielded maleimide end-functionalized heparin with a functionality of 2.2, as characterized by integration of the protons from the maleimide ring compared to the anomeric protons of heparin in ^{1}H NMR spectroscopy (Figure S2), providing sufficient functionality for the modified heparin to act as a crosslinker.

Hydrogels with the thiol- and light-responsive PEG-4-PD-MPA and electrostatic heparin building blocks, respectively, were formed using a Michael-type addition reaction between the sulfhydryl groups of PEG-4-PD-MPA and the maleimide groups of PEG-2-MI and

heparin-MI. The Michael-type addition reaction is a versatile and robust click reaction that occurs readily in aqueous conditions at room temperature.[20] In addition, the reaction does not generate any byproducts, and hence, it has been used widely to design cytocompatible hydrogels.[21] We hypothesized that the rapid chemical crosslinking afforded by this reaction would allow the *in situ* formation of hydrogels upon injection of liquid-gel forming precursors and the encapsulation of bioactive proteins for degradation-mediated release.

In chemically crosslinked hydrogels, the crosslinking reaction plays a crucial role in hydrogel formation and their resulting mechanical properties. In particular, for injectable hydrogels, liquid precursor solutions need to be rapidly polymerized at the site of interest to avoid uncontrolled diffusion of polymers and cargo molecules into the surrounding tissues. Dynamic time sweep experiments were conducted to study hydrogel formation and gelation kinetics. The storage (G') and loss moduli (G'') were recorded for a 7.5 wt% hydrogel composition using a parallel plate geometry, where time sweep measurements were taken within the linear viscoelastic regime (1% strain, 6 rad/s angular frequency). As indicated in the Figure S4, the storage modulus rapidly increased within the initial ~2 minutes from 16 Pa to ~2000 Pa, while no significant change was observed in the loss modulus, indicating the formation of a hydrogel. The crossover point between G' and G'' was not observed before the first data point was acquired, suggesting rapid hydrogel gelation and the potential utility of this material for local injection.

Completion of gelation was achieved after the plateau region was reached, where no significant change in G' was observed between measurements. Post-formation, the storage modulus was significantly higher than the loss modulus as measured by frequency sweeps (0.1 to 100 rad/s) (Figure S4), demonstrating the elastic nature of the network. The modulus observed for these materials is comparable to that of thiol-maleimide hydrogel formulations with lower polymer concentrations (i.e., 5 wt%, G'~2300 Pa).[14] This disparity can be attributed to additional network defects, such as looping or unreacted functional groups, that may be associated with the incorporation of heparin-MI, which significantly impact the crosslink density and ultimately the mechanical properties of the resulting hydrogels.[22] Regardless, our results indicate reproducible and robust hydrogel formation using this Michael-type addition reaction with a gelation time under 30 seconds.

2.2 Hydrogels degrade in response to endogenous and exogenous stimuli

We first investigated the degradation of hydrogels formed with water-stable, aryl-thiol based succinimide thioether linkages, which can undergo a retro-Michael addition in reducing environments, enabling protein release in response to endogenous stimuli. Under non-reducing conditions, the reaction between the aryl-thiol and the maleimide yields a succinimide thioether linkage with the reaction equilibrium directed toward the product. Under reducing conditions, during the reverse reaction, an exogenous thiol, such as that presented by GSH, can react with the maleimide to form a relatively stable alkyl-thiol based succinimide thioether linkage, which is dependent on the pK_a of both the aryl-thiol and the exogenous thiol. The formation of a relatively stable alkyl-thiol based succinimide thioether bond results in the breakage of the original hydrogel crosslink, ultimately leading to network degradation.

After characterizing the modulus of the hydrogel under steady state conditions (e.g., at equilibrium in aqueous solution), we next sought to establish the effect of glutathione concentration on the rate of hydrogel degradation to understand the limits of material responsiveness to an endogenous stimulus. In the human body, the concentration of glutathione varies significantly from the micromolar to the millimolar range;[23] in particular, in tumors, the concentration of thiols varies from 1 to 1.5 mM.[23] Hence, we studied the effects of 0, 1, and 10 mM GSH on the rate of hydrogel degradation. To study hydrogel degradation, we monitored the mechanical properties of hydrogels as a function of time using oscillatory rheometry to assess any decrease in the storage modulus over time that would indicate a decrease in the crosslink density of the hydrogel. The storage modulus at each time point was measured, and the degradation rate was obtained by fitting a plot of the normalized storage modulus as a function of time to first-order degradation kinetics (Fig. 2A). Here, the rate of degradation is proportional to the number of degradable linkages owing to the excess concentration of GSH relative to succinimide thioether linkages. At a concentration of 10 mM GSH, the degradation rate constant was found to be 1.46×10^{-3} min^{-1} ($t_{1/2}$ = 474 min), with complete erosion, or reverse gelation, occurring after 48 hours (2 days). At the lower glutathione concentration (1 mM GSH), the degradation rate constant was found to be 4.47×10^{-4} min^{-1} ($t_{1/2}$ = 1550 min), with complete erosion occurring after 168 hours (7 days). Hydrogels incubated in PBS buffer containing no GSH (i.e., 0 mM GSH) were found to be stable during the experimental time frame (>7 days). Since the glutathione concentration varies significantly *in vivo*, the responsiveness to different glutathione concentrations offers a promising approach to specifically deliver cargo molecules at varied rates for particular sites of interest.

As many therapeutics require doses over different time scales, ranging from a few days to weeks, the ability to easily tune the rate of hydrogel degradation and related therapeutic release profiles is crucial for broad applicability. To simply tune the rate of degradation of the current hydrogels using retro-Michael and thiol exchange reactions, we varied the percent of degradable crosslinks within the hydrogel. Previous studies have demonstrated that alkyl-thiol based succinimide thioether linkages are stable in reducing microenvironments.[14] Hence, the ratio of alkyl-thiol and aryl-thiol within the precursor solution was varied to obtain hydrogels with 33%, 66%, or 100% degradable linkages. Varying the ratio of alkyl to aryl thiols (i.e., stable to GSH-responsive thiols) did not affect the final storage modulus post-formation, indicating that similar crosslinking density was achieved irrespective of the chemical identity of the thiol functional groups. Hydrogels subsequently were incubated in PBS buffer containing 10 mM GSH at room temperature, and the storage modulus was measured at predefined time points. The rate of degradation was calculated by plotting the normalized storage modulus as a function time. As is apparent in Figure 2B, all conditions showed a decrease in the storage modulus, indicating hydrogel degradation in the reducing microenvironment. As noted earlier, the 100% degradable hydrogels showed rapid degradation in a reducing microenvironment with a rate constant of 1.46×10^{-3} min^{-1} and complete erosion occurring after 48 hours (2 days). Hydrogels containing 66% degradable groups exhibited a relatively slower rate of degradation ($k = 6.49 \times 10^{-4}$ min^{-1}), where complete erosion was observed after 96 hours (4 days). The hydrogels containing 33% degradable groups exhibited the slowest degradation among these three

conditions, with a degradation rate constant of 3.59×10^{-4} min^{-1}. These hydrogels did not undergo complete erosion, as this 4-arm PEG network contained fewer than 50% degradable crosslinks, but were too soft to handle and measure mechanically after 120 hours (5 days). These results demonstrate a facile method for controlling degradation kinetics by varying the percentage of degradable crosslinks within the hydrogel.

Although these materials allow GSH-responsive degradation, hydrogel-based drug carriers that degrade in response to multiple triggers, including exogenous stimuli such as externally applied light, would allow spatial and temporal control over drug release for applications in precision medicine.[24] In the present work, incorporation of an *o*-NB moiety into the hydrogel backbone added another handle to control not only the rate of hydrogel degradation, but also the time at which degradation was induced. The effect of externally applied light on the photodegradation of PEG-heparin hydrogels was investigated using cytocompatible doses of long wavelength UV and visible light. In our previous studies, hydrogel degradation was achieved using externally applied light; however, the incorporation of ester bonds caused rapid and uncontrolled ester hydrolysis.[13] The presence of esters in that hydrogel system, consequently, presented significant challenges for future applications in drug delivery, where long-term release (days to weeks) is needed. Hence, we sought to replace the labile ester linkages within the macromers with amide linkages. While the replacement of ester linkages with amide linkages improved the stability of the hydrogel in an aqueous microenvironment, the rate of photodegradation was 2.5 times slower as compared to our previous study ($k_{photodegradation,\ amide} = 0.12\ min^{-1}$, $k_{photodegradation,\ ester} = 0.30\ min^{-1}$ for 10 mW cm^{-2} at 365 nm), as shown in Fig. 2C. A decrease in the rate was expected since typically hydrogels containing *o*-NB groups conjugated to polymers with amide linkages have exhibited slower degradation rates; however, the rate of degradation did not decrease as much as previously reported when using an amide linkage.[25, 26] For example, Anseth and coworkers demonstrated ~15% degradation of an amide-linked photodegradable hydrogel in ~6 minutes using a 10-fold higher light intensity (102 mW/cm^2) than was needed to degrade an ester-linked photodegradable hydrogel network.[25] We hypothesize that the electron-withdrawing nature of the aryl-thiol substituent contributed to the faster degradation rate than typically observed for other amide linked *o*-NB groups.

2.3 Dually responsive hydrogels allow controlled release of a model small bioactive protein FGF-2 in vitro

Growth factor release profiles are of interest in the present work, given our ultimate interest in the controlled delivery of low molecular weight therapeutic proteins. To this end, the release of FGF-2 from PEG-heparin hydrogels was investigated *in vitro*. FGF-2 (~17.2 kDa) is a mitogenic protein that plays a key role in various cellular processes, including cell proliferation, cell migration, wound healing, and endocrine signaling pathways.[9] FGF-2 also has a comparable molecular weight and heparin-binding affinity to that of the immune-activating cytokine IL-2 that is commonly used for the treatment of melanoma by intralesional injection, as outlined in the National Comprehensive Cancer Network guidelines.[17, 18, 27] Both proteins are rapidly degraded in solution, and a controlled drug delivery carrier that retains bioactivity while enabling controlled release *in vivo* could

increase its therapeutic efficacy.[28] In the present studies, FGF-2 loaded hydrogels were incubated in reducing and non-reducing aqueous microenvironments (i.e., PBS buffer containing 10 mM GSH and 0 mM GSH, respectively), and aliquots were removed at pre-determined time points over the course of one week. The concentration of the released FGF-2 subsequently was determined using an enzyme-linked immunosorbent assay (ELISA). The cumulative FGF-2 release was calculated as a function of time as shown in Figure 3A. Under non-reducing conditions, FGF-2 loaded hydrogels exhibited a slight burst release, with approximately 20% of the total FGF-2 released during the experimental time frame. This initial release of FGF-2 can be attributed to passive diffusion of FGF-2 out of the hydrogel, partly driven by the large concentration gradient of FGF-2 between the hydrogel and the sink solution. Notably, under reducing conditions, approximately 40% of the total FGF-2 was released over 3 days, upon which complete erosion of the hydrogel occurred. The continued release of FGF-2 from the hydrogel after the reverse gel point is hypothesized to be continued dissociation of FGF-2 from the heparin monomers after the hydrogel is degraded for a total release of ~90% of loaded FGF-2. The difference in the FGF-2 release profiles for hydrogels in reducing and non-reducing conditions clearly demonstrates that the release of low molecular weight proteins can be tuned by controlling hydrogel degradation. In addition, the electrostatic heparin-protein interaction prevents free diffusion of FGF-2 from the hydrogels after the initial burst release (hydrodynamic radius of FGF-2 = 2.8 nm,[29] estimated mesh size = ~8 nm). Indeed, Kizilel and coworkers reported rapid release of bovine serum albumin (BSA, hydrodynamic radius = 3.56 nm) and glucagon-like peptide (GLP-1, hydrodynamic radius = 1.3 nm) from similar PEG hydrogels.[30] Approximately ~80% of the loaded BSA was released within 3000 min, whereas GLP-1 was released within 300 min, highlighting the importance of heparin-mediated electrostatic interactions for the sustained release of small proteins from PEG-based hydrogels.

Light-mediated hydrogel degradation and subsequent release of FGF-2 was studied to demonstrate the release of FGF-2 over a shorter time period in response to externally applied cytocompatible doses of light (10 mW cm^{-2} at 365 nm). The amount of FGF-2 released from hydrogels was quantified using an ELISA assay. Pristine FGF-2 in solution did not exhibit any significant changes in concentration, as measured via ELISA, when exposed to externally applied UV light (Figure S5), indicating that it remains stable under the dose of light applied. A significant difference in the release profile was observed when hydrogels were irradiated compared to a no light control (Figure 3B). Negligible FGF-2 release was observed during the first 20 minutes of irradiation, consistent with the degradation kinetics of the aryl thiol-based, amide-linked photolabile group as well as the ELISA detection limit. After the reverse gel point was reached for the top layer of the hydrogel (approximately 30 min for this surface eroding, optically-thick hydrogel), continued release of FGF-2 was observed as it dissociates from the free heparin monomers over time. Overall, these results indicate that cargo release can be tuned by application of cytocompatible doses of light.

2.4 Released protein retains bioactivity

FGF-2 is known to promote proliferation of many cell types, including primary human aortic adventitial fibroblasts (AF).[31] Thus, we set out to determine the bioactivity of FGF-2 after encapsulation and release from hydrogels following well-established protocols,[32]

specifically examining the effect of released components on AF proliferation. Hydrogels containing FGF-2 were suspended in reducing and non-reducing microenvironments at 4°C (to minimize protein degradation); after 7 days, the supernatant was lyophilized and reconstituted at a concentration of 1 ng/mL FGF-2 in stromal cell basal medium (SCBM) containing 5% stripped serum. After 48 hours of culture, AFs were treated with 10 μM 5-ethynyl-2-deoxyuridine (EdU) for an additional 24 hrs. AFs cultured in SCBM containing 1 ng/mL fresh pristine FGF-2 were utilized as a positive control, whereas AFs cultures in the absence of FGF-2 served as a negative control. Cell proliferation was quantified by examining the number of EdU-positive AFs after 72 hrs of culture (Figure 4A). AFs treated with released FGF-2 exhibited a proliferation rate of 27%, which was similar to the proliferation rate observed for AFs treated with pristine FGF-2 (Figure 4B). These results indicate that bioactive FGF-2 can be liberated upon stimulation of FGF-2-containing depots.

2.5 Hydrogel degradation mediates release of FGF-2 in vivo

Hydrogel degradation and protein release *in vivo* was subsequently investigated within healthy tissue in mice, which should represent roughly the slowest GSH-responsive release achievable with this system. Specifically, hydrogel precursors were subcutaneously injected for *in situ* hydrogel formation, and the diameter of the resulting hydrogel was monitored over ~2 months. Hydrogels that contained thiol-sensitive linkages showed a decrease in hydrogel diameter, with complete degradation observed by day 25 (i.e., no detectable hydrogel upon palpitation) (Figure 5A). Hydrogels containing alkyl-thiol based succinimide thioether linkages served as a non-degradable control and were stable over the experiment time course (up to 60 days). The slower rate of degradation of the thiol-sensitive hydrogels *in vivo*, in comparison to the rate observed *in vitro* (Figure 2A), likely can be attributed to a lower concentration of GSH within healthy tissues than that probed in the *in vitro* experiments.

FGF-2 labeled with Alexa Fluor 647 (AF-647) was encapsulated within hydrogels during hydrogel formation and its release was tracked over time with fluorescence imaging to evaluate if protein release could be controlled *in vivo* with the degradation of the hydrogel depot. Mice with *in situ* formed hydrogels containing AF-647-labeled FGF-2 were imaged at predetermined time points to monitor the release of FGF-2 from the hydrogel into the surrounding tissue. The total fluorescence intensity within the hydrogel was divided by the area of the hydrogel, and then normalized to the day 0 measurement, for each hydrogel condition. The release of FGF-2 was observed to be more rapid from thiol-sensitive hydrogels (aryl-thiol based linkages) than non-degradable hydrogels (alkyl-thiol based linkages) (Figure 5B). Notably, FGF-2 release was observed to be concatenate with the degradation of the hydrogel in the degradable formulation, whereas its release from the non-degradable formulation over four weeks is controlled strictly by affinity interactions. Differences in total fluorescence within the hydrogels are observed at one week, supporting degradation-mediated release of FGF-2. At longer times, release of FGF-2 from the non-degradable hydrogels is not unexpected given that the FGF-2 should dissociate from heparin over time by affinity-mediated release into the surrounding microenvironment. The relatively faster release of cargo from the degradable hydrogels compared to the non-degradable hydrogels is similar to the trend observed in the *in vitro* experiments.

The radial fluorescence profiles of the hydrogels were also investigated to further understand the release of AF-647-labeled FGF-2 from the different hydrogel compositions (Figure 5C and 5E, representative images Figures 5D and 5F). In the non-degradable hydrogels, we observed a non-significant increase in fluorescence from day 1 to day 6 associated with the inherent variability in the experiment. From day 6 to day 26, the normalized fluorescence intensity decreased from 1.31 to 0.13 at the center of hydrogels, which can be attributed to FGF-2 dissociation from heparin and subsequent diffusion into the surrounding microenvironment.[33] For the 100% degradable hydrogels, a rapid decrease in the normalized fluorescence intensity from 1.00 to 0.12 was observed between day 0 to day 6. This release of protein correlates with the timeframe of hydrogel degradation (Figure 5A). In conjunction with our *in vitro* observations (Figure 3A), these results indicate that protein release likely was driven by both passive and hindered diffusion from the hydrogel upon initial burst and subsequent degradation-mediated mesh size changes, respectively. The normalized intensity value was similar from day 6 to day 26 (0.12 to 0.13, respectively), indicating that most of the loaded protein is released within the first week for the degradable hydrogel condition. Overall, protein release was controlled at short periods (~1–2 weeks) with hydrogel degradation, and at long periods (1 month), complete release of FGF-2 was achieved with either hydrogel formulation. Importantly, the 100% degradable hydrogel composition was completely eroded, providing a mechanism for clearance from the body without surgical removal of the depot.

3. Conclusion

We report the synthesis of water-stable, stimuli-responsive hydrogels in which degradation can be tailored by varying the degradable chemistries that are responsive to reducing microenvironments and externally applied cytocompatible doses of light. Hydrogels were formed rapidly using facile Michael-type reactions and exhibited controlled degradation in the presence of biologically relevant reducing microenvironments (e.g., 1–10 mM GSH) via retro-Michael and subsequent exchange reactions. The rate of hydrogel degradation was found to be dependent on the content of degradable crosslinks and to be responsive to the strength of the reducing microenvironment. Incorporation of an *o*-NB moiety allowed light-triggered hydrogel degradation. Protein release (FGF-2) was controlled by hydrogel degradation by both endogenous and exogenous stimulus *in vitro* (over days to minutes, respectively), up until the reverse gel point. The bioactivity of released FGF-2 was comparable to pristine FGF-2, indicating the ability of the hydrogel to retain the bioactivity of cargo molecules during encapsulation and release. Further, successful hydrogel degradation and FGF-2 release was observed *in vivo* in a murine model. This hydrogel-based, responsive depot is promising for the controlled delivery of FGF-2 in a number of biomedical applications, such as cardiovascular tissue engineering and vascular graft surgeries: release profiles that are sustained (in healthy tissues), responsive (in GSH-enriched tissues), or pulsatile (upon application of light) can be achieved to drive a variety of cellular processes when and where needed.[34] The presented approach could also be easily translated for the release of other heparin-binding proteins of comparable molecular weight and heparin binding affinity, such as the immune activating cytokine IL-2.[17, 18] In summary, the results of our study indicate that incorporation of receptor-host interactions

along with chemistries that respond to endogenous and exogenous stimuli can be utilized to control the release of low molecular weight proteins.

4. Experimental Section

Materials

General organic reagents and solvents were purchased from commercial sources and used as received. 4-arm amine-functionalized poly(ethylene glycol) (PEG-4-NH_2, M_n ~ 10,000 g/mol) and linear maleimide-functionalized poly(ethylene glycol) (PEG-MI, M_n ~ 5,000 g/mol) were purchased from JenKem Technology USA Inc. (Allen, TX). 4-[4-[1-(9-Fluorenylmethyloxycarbonylamino)ethyl]-2-methoxy-5-nitrophenoxy]butanoic acid (Fmoc-PD) was purchased from Advanced ChemTech (Louisville, KY). Deionized water (18 MΩ-cm) was used for experimental procedures. All reactions were conducted in glassware that was oven-dried and cooled while purging with argon. All reactions were performed in duplicate under an inert argon atmosphere using a Schlenk line unless noted otherwise.

Synthesis of aryl-thiol end functionalized PEG

Sulfhydryl groups on MPA were oxidized using hydrogen peroxide in the presence of sodium iodide based on previously published protocol.[35] Briefly, 0.5 g (3 mmol) of MPA was dissolved in 10 mL of ethyl acetate (EtOAc) in the presence sodium iodide (NaI, 4.4 mg, 0.03 mmol) and 30% hydrogen peroxide solution (H_2O_2, 95 mg, 3 mmol, Scheme S3). The solution was stirred at room temperature for 3 hours without inert gas atmosphere. Saturated sodium thiosulfate ($Na_2S_2O_3$) was subsequently added to the reaction mixture (10 mL), and the resulting solution was extracted with EtOAc. The organic phase was isolated and subsequently concentrated by rotary evaporation, and was further purified using silica gel column chromatography (1:1 Hexane:EtOAc).

Purified oxidized MPA (100 mg, 0.6 mmol), HATU (228 mg, 0.6 mmol), and DIPEA (130 mg, 1 mmol) were dissolved in dimethylformamide (DMF) (20 mL), and amine-end functionalized PEG (500 mg, 0.05 mmol) was subsequently added and reacted overnight at room temperature. The reaction solution was precipitated in ethyl ether (10x excess) at 4°C. The precipitated polymer product was separated using centrifugation, and dried polymer was obtained by removal of residual solvents under reduced pressure at room temperature. The polymer was subsequently reduced overnight in the presence of TCEP (470 mg, 1.64 mmol) stirred in DI water (20 mL) at room temperature. The reaction mixture was dialyzed (MWCO 2000 Da) against 3.5 liters of acidic DI water (pH ~ 4 adjusted using hydrochloric acid) with a total of 3 changes over 24 hours at room temperature and then lyophilized to obtain a pale white solid. The degree of thiol functionalization was determined with ^1H NMR spectroscopy (δ 7.19 – 7.13 ppm, Figure S1) using a Bruker AVIII 600 NMR spectrometer (Bruker Daltonics, Billerica, MA) with deuterated DMSO as the solvent.

Synthesis of maleimide functionalized heparin

Low molecular weight heparin was modified with maleimide groups based on previously published protocols.[36] Briefly, 980 mg (0.22 mmol) of heparin (Lovenox®, average molecular weight ~4500 g/mol) was dissolved in 100 mL of 0.1 M 2-(N-

morpholino)ethanesulfonic acid buffer (MES buffer, pH = 6.0). Subsequently, 246 mg (1.46 mmol) of 1-hydroxybenzotriazole hydrate (HOBT), 246 mg of N-(3-Dimethylaminopropyl)-N′-ethylcarbodiimide hydrochloride (EDC, 1.28 mmol), and 246 mg (0.96 mmol) of N-(2-Aminoethyl) maleimide trifuoroacetate salt (AEM) was dissolved and reacted overnight at room temperature under inert atmosphere. The product was subsequently purified using dialysis (MWCO 1000 Da) against 1 M NaCl and deionized water with a total of 3 changes over 48 hours. The reaction mixture was subsequently lyophilized to yield a solid white product. Degree of functionalization (*f = 2.2*) was determined using maleimide protons in downfield region (δ 6.83 ppm, Figure S2) using ^{1}H NMR with deuterated H_2O as the solvent.

Synthesis of aryl-thiol end functionalized photodegradable PEG

Fmoc-PD (200 mg, 0.4 mmol), HATU (152 mg, 0.40 mmol), and DIPEA (104 mg, 0.8 mmol) were dissolved in DMF (10 mL), and amine-end functionalized PEG (500 mg, 1 mmol) was added to the reaction. The reaction solution was stirred overnight at room temperature and subsequently precipitated in ice cold ethyl ether (100 mL). Solid polymer was obtained by filtration and subsequent solvent removal at reduced pressure. The Fmoc group was subsequently removed by dissolving the solid polymer in DMF (30 mL) containing 20% v/v piperidine. The reaction solution was stirred overnight at room temperature; the product was isolated by precipitation (ice cold ethyl ether); and any residual solvent was removed as described earlier. The polymer end functionalized with the photolabile precursor subsequently was reacted with oxidized MPA and purified as described earlier (final purification of aryl-thiol end functionalized PEG: precipitation, filtration, drying, dialysis, and lyophilization) to obtain aryl-thiol end functionalized photodegradable PEG. The degree of functionalization was determined with ^{1}H NMR spectroscopy (δ 7.18 – 7.11 ppm, Figure S3) with deuterated DMSO as the solvent.

Hydrogel formation and rheological characterization

Thiol-functionalized monomers were dissolved in citric acid buffer (pH = 3 prepared using citric acid and disodium phosphate), and maleimide-functionalized monomers were dissolved in phosphate buffered saline (pH = 7). Maleimide-functionalized heparin was mixed with PEG-MI such that 15% of the MI functional groups were contributed by the heparin-maleimide. Thiol-functionalized and maleimide-functionalized monomers were subsequently mixed at 4°C with a 1:1 thiol:maleimide molar ratio to form 7.5 wt% (w/w) hydrogels. For rheological studies, the hydrogels were formed directly on the rheometer (AR-G2, TA Instruments, USA). Mixed precursor solutions were added directly onto a Peltier plate without any apparent increase in the solution viscosity and a 20-mm parallel plate geometry was lowered immediately (120-μm gap). Time sweep measurements were carried out within the linear viscoelastic regime (1% constant strain mode at a frequency of 6 rad s^{-1}) at 25°C. Three independent samples per hydrogel composition were analyzed.

Hydrogel degradation

For hydrogel degradation studies, hydrogels were formed by mixing 7.5 wt% precursor solutions in a cylindrical mold (diameter = 4.6 mm, thickness = 1.8 mm, volume = 30 μL; e.g., 1-mL syringe with the end cut off) at a stoichiometry of 1:1 thiol:maleimide. The

solutions were allowed to gel overnight to ensure maximum possible crosslinking. Resulting hydrogels were washed with PBS (2 mL) and incubated in a reducing microenvironment (1 or 10 mM GSH dissolved in PBS refrigerated until use) at room temperature over the experimental time frame. At predefined time points, the mechanical properties of the hydrogels were assessed using oscillatory rheometry (2 rad/s, 2% strain, 0.25 N force to avoid hydrogel slip) within the linear viscoelastic regime. For light-mediated degradation studies, hydrogels were formed directly on the quartz plate of a UV light accessory (TA Instruments) with a small stoichiometric excess of maleimide (thiol:maleimide ratio = 1:1.1) to avoid any unreacted thiol functional groups. After complete gelation, samples were irradiated with a low dose of long wavelength UV light (10 mW cm^{-2} at 365 nm; Exfo Omnicure Series 2000 light source with 365 nm bandpass filter, SilverLine UV or International Light Radiometer). Storage and loss moduli were simultaneously measured with a 20-mm parallel plate geometry using dynamic time sweep measurements under the linear viscoelastic regime (6 rad/s, 1% strain). Six independent samples per time point were analyzed.

Fibroblast growth factor (FGF-2) release

For growth factor release studies, polymer precursor solutions were mixed along with FGF-2 at a loading concentration of 1 ng μL^{-1} and subsequently pipetted into a cylindrical mold (diameter = 4.6 mm, thickness = 1.8 mm, volume = 30 μL; e.g., 1-mL syringe with end cut off) with. The solutions were allowed to gel at 4°C for 8 hours. Hydrogel discs were washed with PBS thrice to remove any surface-bound FGF-2 and subsequently incubated in 10 mM glutathione in PBS buffer (2 mL volume). The samples were gently shaken on a shaker plate, and 100 μL of sink solution was removed at predetermined time points and replaced with 100 μL of fresh GSH in PBS. The amount of released FGF-2 was quantified using an ELISA assay (Peprotech, Rocky Hill, NJ). The cumulative release at each time point was calculated using following equation:

$$R_t = V_r C_r + \sum_{i=1}^{n} (V_{m_i} C_i)$$

where V_m and V_r indicate the amount of sink solution used for the release measurement and the remaining volume of the sink solution at each time point, respectively (i.e., total volume of the sink, $V = V_r + V_m$); C is the concentration of released FGF-2 obtained using an ELISA assay and the appropriate calibration curve; and i is the number of experimental time points. Four samples per time point were analyzed.

Cell culture

Human aortic adventitial fibroblasts (AFs, unidentified 53 year-old male donor, Lonza) were cultured in stromal cell basal medium (SCBM, Lonza) supplemented with 5% fetal bovine serum (FBS), basic fibroblast growth factor, insulin, and gentamycin/amphotericin-B (all from Lonza). Cells were used between passage numbers 6 and 7 for all assays and maintained at 37°C with 5% CO_2.

Serum stripping

To ensure that the effects on proliferation observed in cell culture experiments were attained solely due to applied FGF-2 (released from hydrogels vs. pristine) and not specific growth factors contained in serum, a HiTrap Heparin Affinity Chromatography column (GE Healthcare, Pittsburgh, PA) was used to strip heparin-binding molecules that are contained within FBS, including FGF-2, following manufacturer's protocol. The column was equilibrated with 50 mL of binding buffer (10 mM sodium phosphate; pH = 6.9). Next, FBS (5 mL) was applied to the column and collected, and the column was further washed with 50 mL of binding buffer. Heparin-binding proteins were then eluted with 50 mL of elution buffer (10 mM sodium phosphate and 1.5 M NaCl, pH = 6.9). The serum was run over the column three times using this process to ensure that heparin-binding molecules were removed. The concentrations of protein in the stripped serum, as well as the wash, binding, and elution solutions, were determined using a Bicinchoninic Acid (BCA) Assay Kit (Pierce, Rockford, IL) performed in triplicate, as described by the manufacturer's instruction.

Proliferation assay to assess the bioactivity of released FGF-2

Hydrogel discs containing FGF-2 were fabricated as described previously and incubated with 10 mM GSH in PBS buffer (2 mL volume). After 7 days, 200 μL of the buffer solution was analyzed by ELISA to determine the amount of FGF-2 released over the culture period. The remainder of the buffer solution was lyophilized to dryness and reconstituted in SCBM containing 5% stripped serum, insulin, and gentamycin/amphotericin-B. Using the results obtained from the ELISA, the lyophilized proteins, which were collected from the buffer the hydrogels were incubated in, were reconstituted at a concentration of 1 ng/mL FGF-2 for comparison to the same concentration of pristine FGF-2 typically used in culture.

AFs were seeded on tissue culture polystyrene 24-well plates at a density of 5×10^3 cells cm $^{-2}$, ensuring an adequate cell density for cell health while achieving limited cell-cell contact to facilitate proliferation. Cells were incubated with SCBM (500 μL) containing 5% stripped serum and 1 ng/mL of FGF-2 that was released from hydrogels. AFs cultured in SCBM containing 5% stripped serum and 1 ng/mL of pristine FGF-2 was utilized as a positive control, whereas AFs cultured in SCBM containing 5% stripped serum in the absence of FGF-2 served as a negative control. After 48 hrs of culture at 37°C, 5-ethynyl-2-deoxyuridine (EdU) was added to the culture medium to achieve a final concentration of 10 μM. AFs were incubated for 24 hours with EdU and subsequently fixed in 4% paraformaldehyde (Electron Microscopy Sciences, Halfield, PA) for 20 minutes, permeabilized in 0.1% Triton-X 100 (Sigma, St. Louis, MO) for 15 minutes, and blocked with 1% BSA in PBS for 1 h. To detect proliferating cells, azide-labeled Alexa Fluor 555 (AF-555, Invitrogen) was conjugated to the alkyne-presenting EdU found within the cell nuclei of proliferating cells by copper-catalyzed azide-alkyne ligation; cell nuclei were counter-stained using Hoescht 33342. Proliferating cells were visualized using an EVOS FL Auto Cell Imaging System (Life Technologies) with 10x objective. The percentage of proliferating cells was calculated from the number of nuclei with incorporated EdU divided by the total number of nuclei multiplied by 100% from five different fields of view per well.

In vivo hydrogel injection and degradation measurement

All experiments were conducted in accordance with the University of California at Davis's Institutional Animal Care and Use. Female C57Bl/6 mice, age 8 weeks, were acquired from The Jackson Laboratory (Bar Harbor Maine). Mice were shaved on their undersides, sterilized with 70% ethanol, and injected subcutaneously with 300 μl of hydrogel precursor solution laden with AF647-labeled FGF-2 for *in situ* depot formation. The diameter of each injected hydrogel was measured daily using calipers. Hydrogels were imaged non-invasively using near infrared imaging (Kodak 2000MM Pro Imaging Station). Specifically, mice were anesthetized using ketamine/xylazine. White light and fluorescence images (Ex625 and Em700 filters, 3-minute exposure) were collected for each mouse at specified time points.

Release of AF-647-labeled FGF-2 from hydrogels in vivo

To assess the release of FGF-2 from injected hydrogels over time, the fluorescence intensity of the collected images were analyzed using the ImageJ 'Measure' function. Specifically, TIFF file images were cropped (400 × 400 pixel box) around the hydrogel area of interest to help remove any background fluorescence present throughout the body of the mouse. Next, the 'default' setting in ImageJ was used to threshold the images to allow for the 'Measure' function to be used to analyze the average fluorescence intensity of the thresholded area of the image. The fluorescence was divided by the hydrogel area (also determined using the 'Measure' function), and subsequently normalized to day 0 for each hydrogel composition. To determine the radial profile of FGF-2 within the hydrogels, a circle was drawn around the hydrogel of interest, the diameter of which was based on the average initial hydrogel diameter for each condition, and the 'Radial Profile' plugin function in ImageJ was used to measure the fluorescence profile over the hydrogel radius. The background fluorescence was subtracted from the measurement, and the data was normalized to the average maximum fluorescent intensity on day 0 for each condition. Four mice were analyzed at each time for each of the hydrogel conditions.

Statistical analysis

Results are expressed as mean ± standard error of mean unless otherwise specified. Specific numbers of replicates ($n \geq 3$) are noted for each experiment within the Results and Discussion. Statistical significance was analyzed by performing a Student's t-test, where $p < 0.05$ was considered significant. SigmaPlot and Microsoft Excel were utilized for data processing and statistical analysis.

Supplementary Material

Refer to Web version on PubMed Central for supplementary material.

Acknowledgments

The authors are grateful to Dr. Robert E. Akins, Jr. (Nemours - Alfred I. duPont Hospital for Children, Wilmington, DE) for providing low molecular weight heparin and human aortic adventitial fibroblasts. Research reported in this publication was supported by an Institutional Development Award (IDeA) from the National Institute of General Medical Sciences (NIGMS) of the National Institutes of Health (NIH) (P20GM103541), an IDeA from NIGMS from the NIH (1 P30 GM110758-01), the Burroughs Wellcome Fund (1006787), a National Science Foundation (NSF) CAREER Award (DMR-1253906), the Pew Charitable Trusts (00026178), and the University of Delaware

Research Foundation. EM was supported by funding from CIRM (RN3-06460) and the NIH (1DP2OD008752 and 3P30CA093373). PMK would like to thank the Sigma Xi grant-in-aid research funding for additional support. We also thank the Servier Medical Art for the use of a vector image template.

References

1. Kharkar PM, Rehmann MS, Skeens KM, Maverakis E, Kloxin AM. ACS Biomater Sci Eng. 2016; 2:165. [PubMed: 28361125]
2. Annabi N, Tamayol A, Uquillas JA, Akbari M, Bertassoni LE, Cha C, Camci-Unal G, Dokmeci MR, Peppas NA, Khademhosseini A. Advanced materials. 2014; 26:85. [PubMed: 24741694] Kharkar PM, Kiick KL, Kloxin AM. Chemical Society reviews. 2013; 42:7335. [PubMed: 23609001]
3. Gilbert T, Smeets NM, Hoare T. ACS Macro Letters. 2015; 4:1104.
4. Yesilyurt V, Webber MJ, Appel EA, Godwin C, Langer R, Anderson DG. Advanced materials. 2016; 28:86. [PubMed: 26540021]
5. Lin CC, Anseth KS. Pharmaceutical research. 2009; 26:631. [PubMed: 19089601]
6. Holloway JL, Ma H, Rai R, Burdick JA. Journal of controlled release : official journal of the Controlled Release Society. 2014; 191:63. [PubMed: 24905414] Jiang Y, Chen J, Deng C, Suuronen EJ, Zhong Z. Biomaterials. 2014; 35:4969. [PubMed: 24674460] Chen J, Zou Y, Deng C, Meng F, Zhang J, Zhong Z. Chem Mater. 2016; 28:8792.Liang Y, Kiick KL. Biomacromolecules. 2016; 17:601. [PubMed: 26751084]
7. Chen J, Zou Y, Deng C, Meng F, Zhang J, Zhong Z. Chemistry of Materials. 2016; 28:8792.
8. Purcell BP, Lobb D, Charati MB, Dorsey SM, Wade RJ, Zellars KN, Doviak H, Pettaway S, Logdon CB, Shuman JA, Freels PD, Gorman JH 3rd, Gorman RC, Spinale FG, Burdick JA. Nature materials. 2014; 13:653. [PubMed: 24681647]
9. Rifkin DB, Moscatelli D. The Journal of cell biology. 1989; 109:1. [PubMed: 2545723]
10. Bakaic E, Smeets NMB, Hoare T. RSC Advances. 2015; 5:35469.
11. Vulic K, Shoichet MS. Biomacromolecules. 2014; 15:3867. [PubMed: 25230248] Yamaguchi N, Kiick KL. Biomacromolecules. 2005; 6:1921. [PubMed: 16004429] Zhang L, Furst EM, Kiick KL. Journal of controlled release : official journal of the Controlled Release Society. 2006; 114:130. [PubMed: 16890321]
12. Liang Y, Kiick KL. Acta biomaterialia. 2014; 10:1588. [PubMed: 23911941]
13. Kharkar PM, Kiick KL, Kloxin AM. Polym Chem. 2015; 6:5565. [PubMed: 26284125]
14. Kharkar PM, Kloxin AM, Kiick KL. J Mater Chem B. 2014; 2:5511. [PubMed: 25908977]
15. Kloxin AM, Kasko AM, Salinas CN, Anseth KS. Science. 2009; 324:59. [PubMed: 19342581]
16. Nie T, Baldwin A, Yamaguchi N, Kiick KL. Journal of controlled release : official journal of the Controlled Release Society. 2007; 122:287. [PubMed: 17582636] Yamaguchi N, Zhang L, Chae BS, Palla CS, Furst EM, Kiick KL. Journal of the American Chemical Society. 2007; 129:3040. [PubMed: 17315874] Zieris A, Prokoph S, Levental KR, Welzel PB, Grimmer M, Freudenberg U, Werner C. Biomaterials. 2010; 31:7985. [PubMed: 20674970]
17. Thompson LD, Pantoliano MW, Springer BA. Biochemistry. 1994; 33:3831. [PubMed: 8142385]
18. Najjam S, Gibbs RV, Gordon MY, Rider CC. Cytokine. 1997; 9:1013. [PubMed: 9417813]
19. Ashikari-Hada S, Habuchi H, Kariya Y, Kimata K. The Journal of biological chemistry. 2005; 280:31508. [PubMed: 16027124]
20. Mather BD, Viswanathan K, Miller KM, Long TE. Prog Polym Sci. 2006; 31:487.Nair DP, Podgórski M, Chatani S, Gong T, Xi W, Fenoli CR, Bowman CN. Chem Mater. 2014; 26:724.
21. Fu Y, Kao WJ. Journal of biomedical materials research Part A. 2011; 98:201. [PubMed: 21548071] Liu ZQ, Wei Z, Zhu XL, Huang GY, Xu F, Yang JH, Osada Y, Zrinyi M, Li JH, Chen YM. Colloids and surfaces. B, Biointerfaces. 2015; 128:140. [PubMed: 25744162] Yu Y, Deng C, Meng F, Shi Q, Feijen J, Zhong Z. Journal of biomedical materials research Part A. 2011; 99:316. [PubMed: 21887740]
22. Shibayama M. Soft Matter. 2012; 8:8030.Treloar, LRG. The physics of rubber elasticity. Oxford University Press; 1975.

23. Rossi R, Milzani A, Dalle-Donne I, Giustarini D, Lusini L, Colombo R, Di Simplicio P. Clinical chemistry. 2002; 48:742. [PubMed: 11978601]
24. Mura S, Nicolas J, Couvreur P. Nature materials. 2013; 12:991. [PubMed: 24150417] Wang X, Wang C, Zhang Q, Cheng Y. Chemical communications. 2016; 52:978. [PubMed: 26588349]
25. McKinnon DD, Brown TE, Kyburz KA, Kiyotake E, Anseth KS. Biomacromolecules. 2014; 15:2808. [PubMed: 24932668]
26. Shin DS, You J, Rahimian A, Vu T, Siltanen C, Ehsanipour A, Stybayeva G, Sutcliffe J, Revzin A. Angewandte Chemie. 2014; 53:8221. [PubMed: 24931301]
27. Shi VY, Tran K, Patel F, Leventhal J, Konia T, Fung MA, Wilken R, Garcia MS, Fitzmaurice SD, Joo J. J Am Acad Dermatol. 2015; 73:645. [PubMed: 26259990] Maverakis E, Cornelius LA, Bowen GM, Phan T, Patel FB, Fitzmaurice S, He Y, Burrall B, Duong C, Kloxin AM. Acta Derm Venereol. 2015; 95:516. [PubMed: 25520039]
28. Jeon O, Ryu SH, Chung JH, Kim BS. Journal of controlled release : official journal of the Controlled Release Society. 2005; 105:249. [PubMed: 16088988]
29. Onuma K, Kanzaki N, Kobayashi N. Macromolecular bioscience. 2004; 4:39. [PubMed: 15468286]
30. Bal T, Kepsutlu B, Kizilel S. Journal of biomedical materials research Part A. 2014; 102:487. [PubMed: 23505227]
31. Boilly B, Vercoutter-Edouart A, Hondermarck H, Nurcombe V, Le Bourhis X. Cytokine Growth Factor Rev. 2000; 11:295. [PubMed: 10959077]
32. Bae KH, Lee F, Xu K, Keng CT, Tan SY, Tan YJ, Chen Q, Kurisawa M. Biomaterials. 2015; 63:146. [PubMed: 26100344]
33. Lin CC, Metters AT. Adv Drug Deliv Rev. 2006; 58:1379. [PubMed: 17081649]
34. Rufaihah AJ, Seliktar D. Adv Drug Deliv Rev. 2016; 96:31. [PubMed: 26212158] Akintewe OO, Roberts EG, Rim NG, Ferguson MA, Wong JY. Annu Rev Biomed Eng. 2017
35. Kirihara, Masayuki, Asai, Yasutaka, Ogawa, Shiho, Noguchi, T., Hatano, A., Hirai, Y. Synthesis. 2007; 21:3286.
36. Baldwin AD, Robinson KG, Militar JL, Derby CD, Kiick KL, Akins RE. Journal of biomedical materials research Part A. 2012; 100:2106. [PubMed: 22615105] Baldwin AD, Kiick KL. Polym Chem. 2013; 4:133. [PubMed: 23766781]

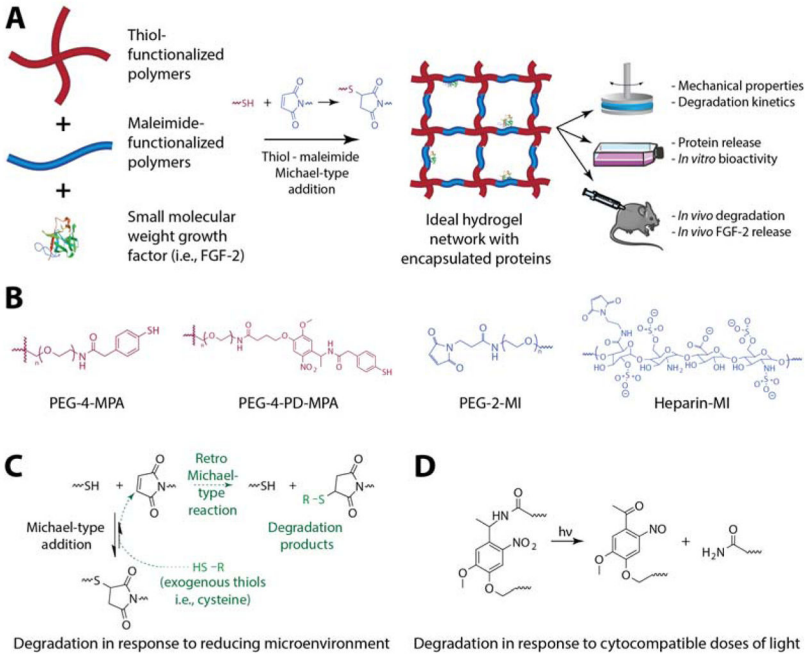

Fig 1. Polymeric building blocks for hydrogel formation

A) Reducing-microenvironment- or light-sensitive hydrogels were formed by reacting **B)** an aryl-thiol end functionalized poly(ethylene glycol) macromolecular precursor (PEG-4-MPA) or a photodegradable aryl-thiol end functionalized PEG (PEG-4-PD-MPA) with a maleimide-end functionalized PEG (PEG-2-MI) and a maleimide functionalized low molecular heparin (Heparin-MI) via a Michael-type reaction in an aqueous microenvironment. Low molecular weight proteins, such as growth factors (FGF-2 in the present study), cytokines, and immunomodulatory agents, can be incorporated within the hydrogel during network formation utilizing heparin-associated receptor-ligand interactions for protein retention. **C)** Aryl-thiol based succinimide thioether linkages exchange with free thiols in solution leading to the formation of a relatively stable alkyl-thiol (i.e., cysteine) based succinimide thioether linkage, resulting in hydrogel degradation. **D)** The photolabile *o*-nitrobenzyl moieties undergo irreversible photoisomerization in response to cytocompatible doses of long wavelength UV or visible light, yielding ketone and amide products.

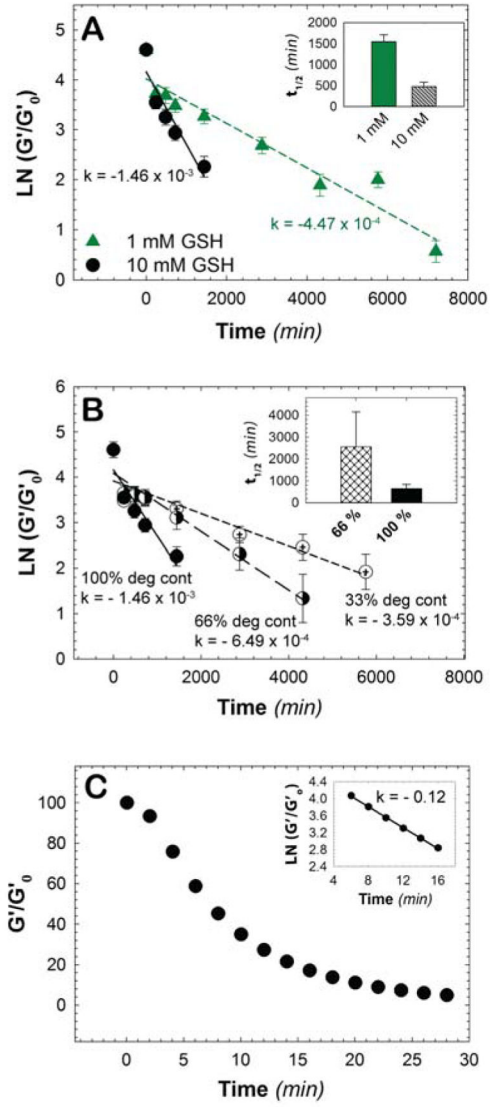

Fig. 2. Stimuli-responsive hydrogel degradation

A) The rate of hydrogel degradation was found to be responsive to glutathione (GSH) concentration. In a high reducing microenvironment (10 mM), like that found intracellularly, the rate of degradation was an order of magnitude faster when compared to a lower reducing microenvironment (1 mM) like that within carcinoma tissues, indicating the promise of this approach for reducing-microenvironment sensitive therapeutic release. The degradation half-lives of hydrogels exposed to different concentrations of GSH were found to be 474 minutes and 1550 minutes for high and low concentrations of GSH, respectively. **B)** Using different ratios of alkyl to aryl thiols, the number of degradable crosslinks was varied between 33% to 100%, which in turn controlled the rate of bulk hydrogel degradation. The degradation half-life was found to be approximately 2550 minutes and 635 minutes for 66% and 100% degradable hydrogels, respectively; the 33% degradable hydrogel, as expected, did not undergo complete degradation. **C)** Photodegradable MPA-based hydrogels undergo degradation in response to externally applied light (10 mW/cm^2 at 365 nm). The rate of

photodegradation was evaluated in the linear region between 6 to 16 minutes, yielding a rate constant of 0.12 min^{-1} for photocleavage and degradation half-life of approximately 8.3 min for hydrogels irradiated with low intensity, long wavelength UV light. The data shown illustrate the mean ($n \geq 3$) with error bars showing the standard error.

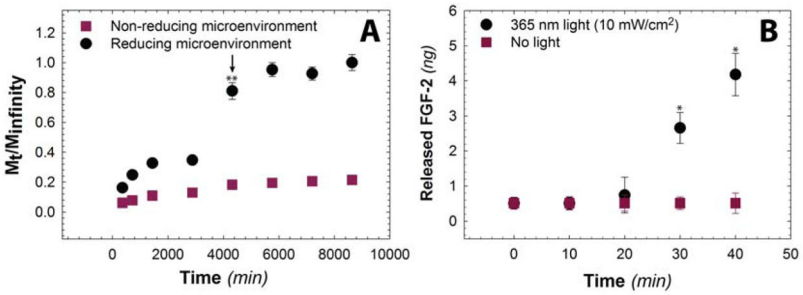

Fig. 3. Degradation-mediated release of model small bioactive protein

A) Release of FGF-2 in response to a reducing microenvironment was monitored *in vitro* using an enzyme-linked immunosorbent assay (ELISA) (reducing microenvironment: PBS buffer containing 10 mM GSH; control: non-reducing microenvironment PBS buffer). Hydrogels exhibit minimal burst release in the non-reducing microenvironment. In contrast, under the reducing microenvironment, FGF-2 was released rapidly, with approximately ~40% of cargo released before complete erosion (i.e., reverse gelation, noted with arrow at 4300 minutes), and ~80–95% was released upon complete hydrogel degradation. Upon hydrogel dissolution at 4300 minutes, the amount of FGF-2 released under the reducing microenvironment was statistically significant compared to FGF-2 released under the non-reducing microenvironment. **B)** Release of FGF-2 in response to cytocompatible, clinically-relevant light doses (10 mW cm^{-2} at 365 nm) was monitored using an ELISA. A statistically significant increase in FGF-2 release was observed with irradiation times sufficient for light-mediated erosion of the surface of the hydrogel in comparison to the control (no light). The data shown illustrate the mean ($n \geq 4$) with error bars showing the standard error. * indicates $p < 0.05$, ** indicates $p < 0.001$.

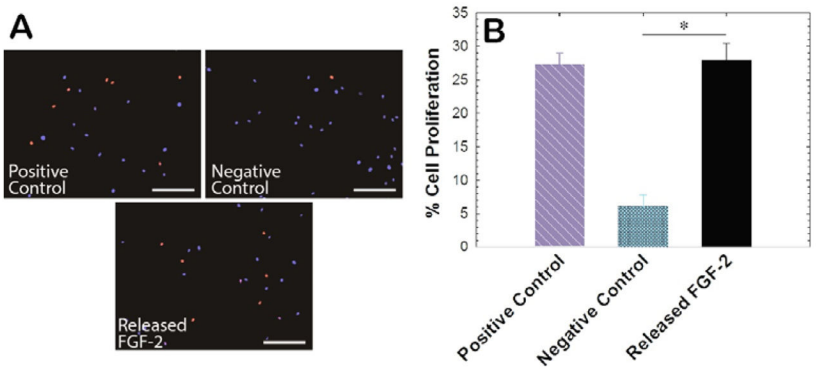

Fig. 4. Bioactivity of released FGF-2

A) Bioactivity of FGF-2 that was released from PEG-heparin hydrogels was studied *in vitro* using an adventitial fibroblast (AF) proliferation assay, as FGF-2 is known to promote cell proliferation. FGF-2 that was released from the hydrogels was added to AFs during *in vitro* cell culture, and proliferating cell nuclei were labeled with Alexa Fluor 555 (red) using an EdU assay (scale bar, 200 μm). **B)** Released FGF-2 demonstrated a similar effect on cell proliferation as pristine FGF-2 added at a similar concentration (positive control) relative to cells in growth medium alone (negative control), indicating that the protein bioactivity was not affected during the encapsulation and subsequent release process. Data shown illustrate the mean ($n \geq 4$) with error bars showing the standard error. * indicates $p < 0.05$.

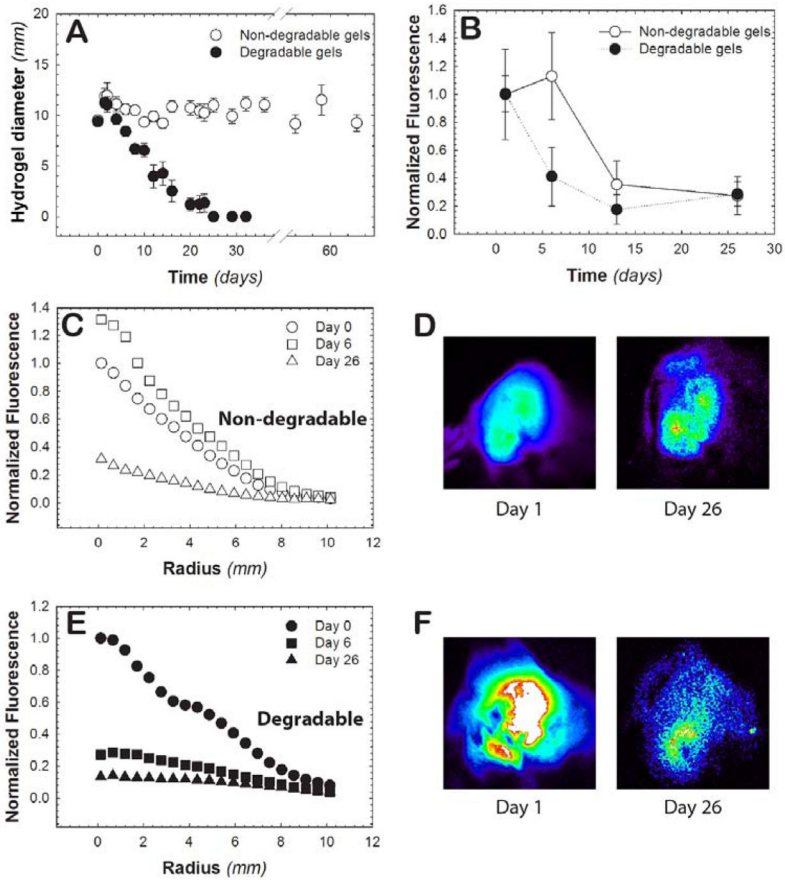

Fig. 5. *In vivo* hydrogel degradation

A) The ability of hydrogels to degrade *in vivo* was monitored in a mouse model. After subcutaneous injection, the hydrogel diameter was measured with calibers to monitor the change in the size of the hydrogels over a 60-day time course. At 25 days, no hydrogel was detectable upon palpitation for the 100% degradable hydrogels, whereas little change in size was observed for the non-degradable control hydrogel. **B)** The fluorescence of injected hydrogels containing fluorescently-labeled FGF-2 was monitored for 26 days post injection. The total fluorescence was divided by the area of the hydrogel and subsequently normalized to the average fluorescence on day 0. The radial distribution of FGF-2 from **C)** non-degradable (open markers) and **E)** degradable hydrogels (closed markers) was determined to monitor FGF-2 release from the hydrogel network. Representative images of these hydrogels are shown for day 1 and day 26 for **D)** non-degradable and **F)** degradable hydrogel formulations. Taken together, FGF-2 release was observed to be concatenate with the degradation of the hydrogel for the degradable formulation, whereas its release was controlled strictly by affinity interactions for the non-degradable formulation over four weeks. Data shown illustrate the mean ($n \geq 3$) with error bars showing the standard error.